ORIGINAL PAPER

Flow Injection Small-volume Fiber-optic pH Sensor Based on Evanescent Wave Excitation and Fluorescence Determination

Yan Xiong · Ying Huang · Zhongbin Ye · Yafeng Guan

Abstract A small-volume fiber-optic pH sensor (FOEWS) based on evanescent wave excitation is developed and evaluated. The sensor is simply fabricated by inserting a decladded optical fiber into a transparent capillary tube. A microchannel between the optical fiber and the capillary inner wall was formed and acted as flow cell for solution flowing through. The pH-sensitive fluorophore of fluorescein can be excited by the evanescent wave field produced on the fiber core surface to produce emission fluorescence. pH value was then sensed by its enhancing effect on the emission fluorescence intensity. The response range of the sensor is from pH 2.09 to pH 8.85 and the linear range is from pH 3.25 to 8.85. The proposed sensor has a small detection volume of 2.5 μL and a short response time of 8 s. It has been applied to measure pH values of real water samples and was in good agreement with the results obtained by commercial pH meter.

Y. Xiong · Z. Ye
State Key Laboratory of Oil and Gas Reservoir Geology and Exploitation, Southwest Petroleum University, Chengdu 610500, China

Y. Xiong · Y. Huang · Z. Ye
School of Chemistry and Chemical Engineering, Southwest Petroleum University, Chengdu 610500, China

Y. Guan (✉)
Department of Instrumentation and Analytical Chemistry, Dalian Institute of Chemical Physics, Chinese Academy of Sciences, Dalian 116023, China
e-mail: guan_yafeng@yahoo.com.cn

Introduction

The pH measurement is of great importance in various areas of industry, medical environmental and process monitoring [1–4]. So far, many approaches have been developed for constructing pH sensors [5–15]. Among these methods, the preparation of fiber optic pH sensors has attracted much research effort. For remote and real time monitoring in some hazardous environments [16], fiber optic pH sensors may offer certain advantages over other types of sensors due to their advantages such as small size, good flexibility, multiplexing capability, low propagation loss and resistance to electromagnetic interference [17].

In recent years, fiber-optic evanescent wave sensor (FOEWS), which avoids laborious optical adjustment, has been conveniently and effectively used in many practical applications [18–20]. When light transmitted by total internal reflection (TIR) in the optical fiber, evanescent wave (EW) field could be produced on the fiber core surface. The EW could penetrate into the surrounding medium and directly or indirectly interact with analytes. In our previous work, we have developed several FOEWS for the determinations of gas oxygen, dissolved oxygen and nitrite [21–24].

Fluorescence detection, which has obvious advantages of high sensitivity and selectivity [25, 26], has been widely utilized for the construction of pH sensors. Though several other fluorescence measurement methods, including lifetime measurement [11, 27], ratiometric dual-wavelength measurement [28–30], and photoinduced electron transfer (PET) measurement [31] have been developed, fluorescence intensity measurement [32–34] is still one of the most widely employed analytical techniques. This is mainly because the intensity measurement has no demand on sophisticated instrumentations, has no lost of spectral information, and generally does not need fluorophore receptor.

In this paper, we design a fiber-optic evanescent wave pH sensor with small detection volume using fluorescence intensity detection combined with flow-injection analysis. The sensor was simply fabricated by inserting a decladded optical fiber into a transparent capillary tube. A microchannel between optical fiber and the capillary inner wall was formed as flow cell for solution flowing though. The pH-sensitive fluorophore of fluorescein could be excited by evanescent wave field produced on the fiber core surface when flowing through the microchannel. The produced fluorescence emission was detected by the detector set on the capillary side and H$^+$ could be sensed by its enhancing effect on the fluorescence intensity. A broad response range from pH 2.09 to pH 8.85 was obtained. The performance of the designed pH sensor was studied and applied to real water samples including tap water, purified water and green tea water.

Theory

The sensor configuration designed was based on the interaction between evanescent wave (EW) and an analyte-sensitive reagent. The EW is the exponentially decaying electric field that penetrates a short distance into the low index medium when total internal reflection (TIR) occurs at a dielectric interface. The degree of penetration is often characterized by the penetration depth, d_p, which is the perpendicular distance from the interface to where the electric field amplitude, E, falls to $1/e$ of its value at the interface (E$_0$) [35].

$$E = Eo \exp(-z/d_p) \qquad (1)$$

The penetration depth, d_p, of the evanescent field is defined as

$$d_p = \lambda/[2\pi(n_1{}^2\sin^2\theta - n_2{}^2)^{1/2}]$$
$$= \lambda/[2\pi(n_1{}^2\sin^2\theta - \sin^2\theta_c)^{1/2}] \qquad (2)$$

where λ is the wavelength of the radiation, θ is the incident angle, θ_c is critical angle, n_1 and n_2 are the refractive index of the dense and rare media, respectively. Fluorescent molecules present within the penetration depth of the evanescent field can be excited by the evanescent wave, resulting in fluorescence emission.

Experimental

Reagents and Materials

Fluorescein was obtained from Sigma, USA. Boric acid (H$_3$BO$_4$), phosphoric acid (H$_3$PO$_4$), and acetic acid (HAC)

were purchased from Kaiyuan Chemical Reagent Company (Tieling, China), Tianjing Kemael Chemical Reagents Development Center (Tianjing, China), and Shenyang Chemical Reagent Company (Shenyang, China), respectively. The Britton-Robinson buffer solutions (denoted as BR buffer solution hereafter) in the pH range of 2.0–11.5 were prepared by mixing 0.04 mol L^{-1} H$_3$PO$_4$, H$_3$BO$_4$, and HAC, then adjusting the desired pH value by adding different volume 0.2 mol L^{-1} of NaOH. Beyond the pH range, the buffer solution was adjusted by addition of concentrated HCl or NaOH solution.

Fluorescein stock solution of 2×10^{-3} mol L^{-1} was prepared in ethanol and working solutions were prepared freshly with Wahaha® purified water (Wahaha, Hangzhou, China) for daily use. All other chemicals were at least of analytical grade. Wahaha® purified water was used for the preparation of solutions and throughout the experiments.

The plastic-clad silica (PCS) optical fiber (inner diameter=300 μm, NA=0.37) was purchased from Chunhui Inc., Ltd. (Nanjing, China). The silica capillary tube (inner diameter=530 μm, outer diameter=690 μm) was purchased from Yongnian Optic Fiber Plant (Hebei, China).

Apparatus

A blue lamp LED (Shifeng Corp., Shenzhen, China) was used as light source. A photomultiplier tube (PMT R928, Hamamatsu, Japan) was used as detector for the fluorescence intensity measurement. An interference filter (BP 530 nm; FWHM 30 nm; Huibo Optical Corp. Ltd., China) was used for fluorescence passing through.

A spectrometer (USB4000, Ocean Optics, USA) was used for the spectral measurement of the LED light source. A UV-Vis spectrometer (lambda 35, Perkin Elmer, USA) was used for the UV-Vis absorption spectral measurements. All the pH calibration measurements were carried out on a pH meter (PHSJ-3F, Shanghai, China). A microinfusion pump (WZS–50FZ, Zhejiang university medical instrument Co., Ltd., China) was used to deliver the water carrier and the sensing reagents. Injection was performed using a six-port injection valve (Valco Instruments, USA).

Construction of the Small-volume Sensor

First, part of the polyimide coating (20 mm in length) on the capillary was burned off to form a detection window and part of the plastic clad (20 mm in length) was decladded to let evanescent wave can penetrate out. Then the sensor was constructed by inserting the optical fiber into the capillary tube. To reduce friction and damage to the surface of the fiber, the capillary tube was filled with water before the insertion process. An annular microchannel was formed as flow cell for solutions flowing through.

The blue LED light source was coupled with one end of optical fiber and the PMT was set along the capillary on the side of the fiber. As a result, the PMT optical window surface was designed to be parallel to the axis of the optical fiber and the distance between them was fixed to 15.5 mm. PTFE tubing (0.4 mm i.d.) was used to connect all components in the flow system. As shown in Fig. 1, the water carried the samples and mixed with the pH-sensitive solution of fluorescein through a stainless steel "T" connection. Then the mixture flowed through the micro-channel and excited by the evanescent wave to produce fluorescence.

Results and Discussion

Spectral Characteristics

The spectrum (A) in Fig. 2(a) is the UV-Vis absorption spectrum of fluorescein, which is used as pH-sensitive dye in the proposed sensor. It can be seen that fluorescein has a Q band at 450 nm (λ_{abs}=450 nm). The emission spectrum of the blue LED chosen as light source (the spectrum (B) in Fig. 2(a)) shows a center wavelength at 462 nm, which is well-overlapped with the absorption spectrum of fluorescein. Figure 2(b) shows fluorescence emission of fluorescein at 520 nm (λ_{em}=520 nm) excited by LED. Therefore, it was appropriate to choose a blue LED as the excitation light source for the proposed fiber-optic evanescent-wave fluorescence sensor.

Concentration Optimization

To obtain the maximum light collection efficiency, the sensing length of the optical fiber was selected to be 20 mm to match the length of the optical window of PMT. The microchannel formed between the fiber and the capillary tube had a whole volume <6 μL with 2.8 μL in front of the PMT window. This small volume could effectively speed up the solution displacement and shorten the response time at a fixed flow rate. Meanwhile, the narrow d_c (115 μm) of the microchannel could effectively inhibit the sample
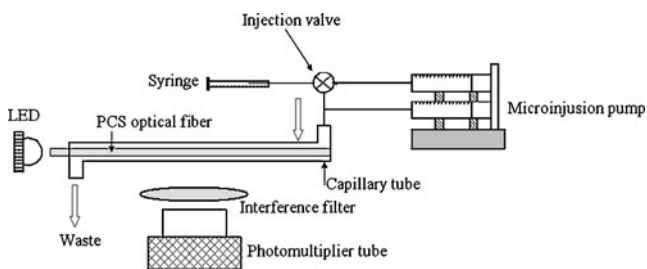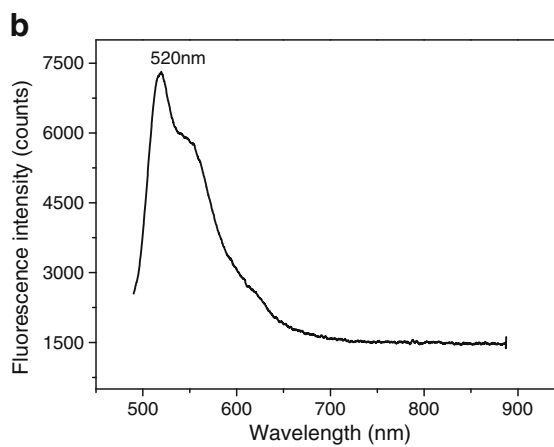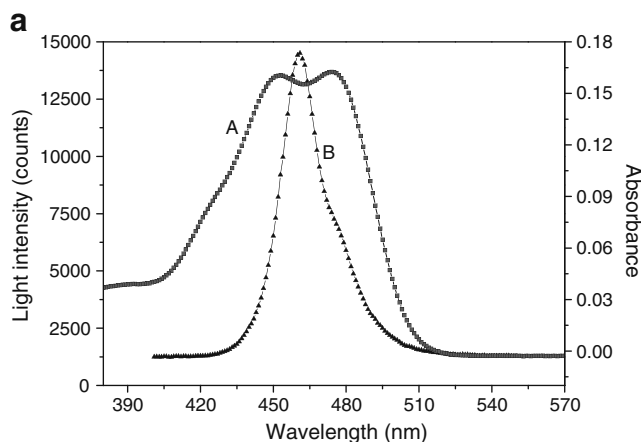

Fig. 2 **a** UV-Vis absorption spectrum of fluorescein (spectrum A) and emission spectrum of the blue LED light source (spectrum B). **b** Fluorescence emission of fluorescein illuminated by the chosen LED

Fig. 1 Schematic drawing of the small-volume FOEWS arrangement

dispersion caused by solution mixing and improve the sensor sensitivity. In order to obtain the best analytical performance of the proposed FOEWS system, several operation conditions were optimized. The sample used during the optimization was BR suffer solution with pH=6.

First, sample volume was investigated by starting from 3 μL to 110 μL while flow rates of water carrier and 5×10^{-5} mol L^{-1} fluorescein solution were both kept constant at 200 μL min^{-1}. It was observed that, with sample volumes greater than 20 μL, the fluorescence did not increase substantially. Thus, 20 μL was chosen as the optimal sample volume.

Second, fluorescein concentration was optimized by measuring the ratio of the fluorescence signal to noise (S/N) with fluorescein concentrations from 1×10^{-6} to 5×10^{-4} mol L^{-1}. The flow rates of fluorescein solution and water carrier were both also kept constant at 200 μL min^{-1}. The results showed that the fluorescence emission intensity of both fluorescein and the background increased with higher concentration. The maximum S/N ratio was obtained

with 1×10^{-4} mol L^{-1} fluorescein, which was selected for the subsequent experiments.

Third, the flow rate of fluorescein was investigated from 50 to 300 μL min^{-1} with water carrier at 200 μL min^{-1}. Results showed that fluorescence intensity increased with increasing the flow rate, while the background noise also increased. The maximum S/N was found at flow rate of 200 μL min^{-1}.

At last, the flow rate of water carrier was also tested from 50 to 300 μL min^{-1}. With obtaining proper S/N and enough response time, 200 μL min^{-1} was finally chosen as the optimal rate for water carrier.

Analytical Performance

The pH response of the proposed sensor was tested with flow-injection analysis in the range from 1.71 to 9.91 as shown in Fig. 3. It was found that the proposed sensor made good response to a broad range of pH from 2.09 to 8.85. When pH >8.85 or pH <2.09, no obvious change of fluorescence intensity could be observed ($P > 0.05$). The linear pH range of the sensor was from 3.29 to 8.85 and the regression equation was $I = 33.99$ pH-94.171 with a correlation coefficient of 0.9815, where I was the fluorescence intensity. The characteristic calibration curve of the sensor is shown in Fig. 4 and the inset shows the linear calibration curve from pH 3.28 to pH 8.85.

Effect of Ionic Strength

The sensitivity to ionic strength was a major factor to limit the practical application of optical pH sensors for real samples. In this work, the effect of ionic strength on the pH sensor was also examined by replacing the water carrier with 0.05, 0.1 and 0.5 mol L^{-1} NaCl solutions, respectively.
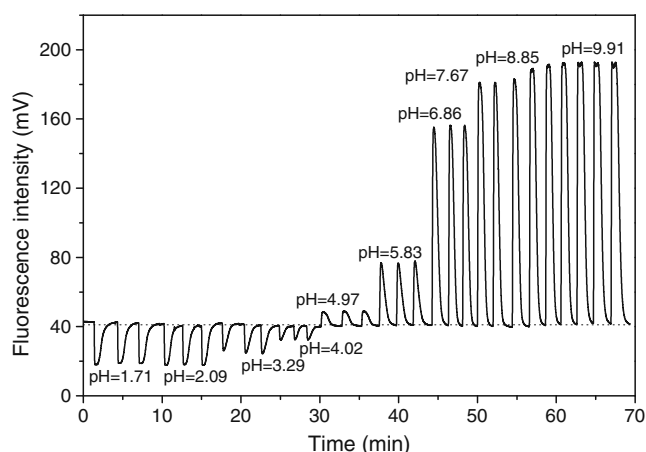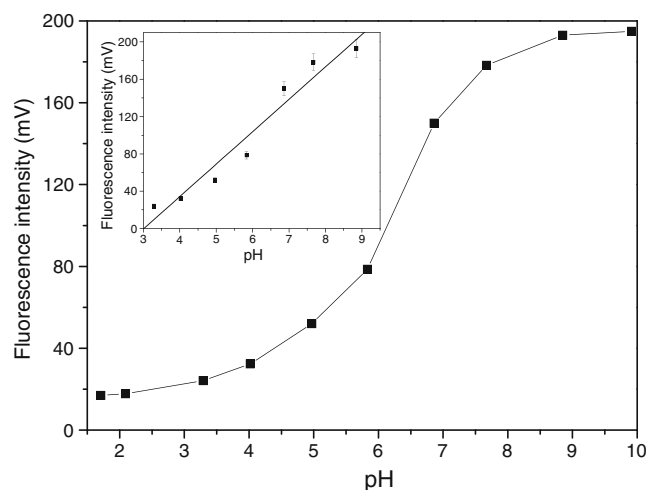

Fig. 4 Calibration curve of the sensor. The inset shows the linear calibration curve from pH 3.28 to pH 8.85

As shown in Fig. 5, with increasing ionic strength from 0.05 to 0.5 mol L^{-1}, the apparent pKa value changed slightly from 6.36 to 6.51. This result shows that changes in ionic strength only affect the pKa value of 0.15 pH units, indicating that the present sensor was resistive to ionic strength.

Interference Study

Under the chosen conditions and using the manifold depicted in Fig. 1, the interference of some species commonly present in water was examined by analyzing the BR solution with pH=6.5. The tolerable limit of foreign species was considered with the relative error less than 5%. The results are listed in Table 1. As could be seen, most of ions tested did not interfere with determination.
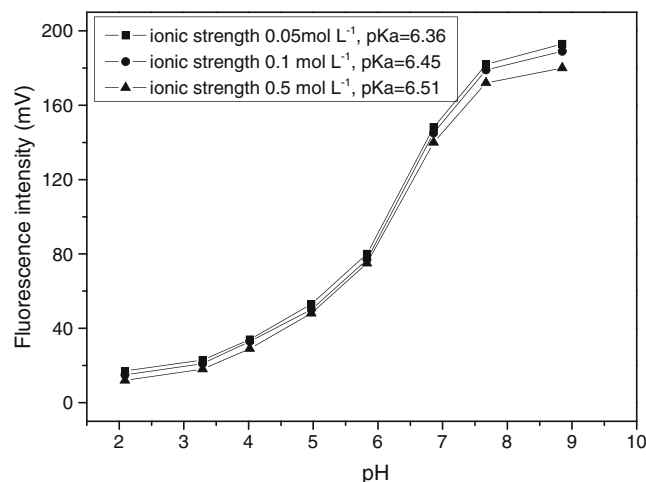

Fig. 3 Response curve of the sensor in the range between pH 1.71 and pH 9.91

Fig. 5 Effect of ionic strength on the pH sensor

Table 1 Interference of foreign ions

Interference ions	Tolerance limit ($\times 10^{-3}$ mol L^{-1})
NO_3^-	5.0
Cl^-	3.0
SO_4^{2-}	2.5
PO_4^{3-}	2.0
HCO_3^-	2.0
CH_3COO^-	1.5
CO_3^{2-}	1.0
Ca^{2+}	2.0
Zn^{2+}	2.0
Mn^{2+}	1.5
Co^{2+}	1.0
Ni^{2+}	1.0
Cu^{2+}	0.5
Fe^{3+}	0.5

Repeatability and Response Time

The repeatability of the sensor was studied using BR buffer solution with pH=6.5. Figure 6 shows the typical response obtained by injecting the selected BR buffer solutions successively. The relative standard deviation (R.S.D.) was 1.2% (n=7).

The response time was a key factor to evaluate a sensor. A short response time was generally required for most applications. The parameter used to characterize response time was the so-called t_{90}, which was the time at which 90% of the maximum signal occured. In this work, relative short t_{90} of approximate 8 s was obtained with a recovering time approximate 55 s. These times remained the same no matter whether one switched from low to high concentration or the reverse. The fast response of the proposed sensor probably resulted from the small-volume microchannel
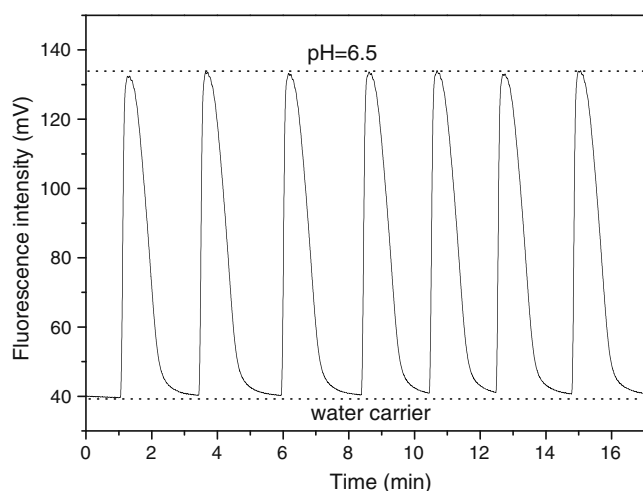
Fig. 6 Sensor repeatability measured at pH 6.5

with narrow d_c (115 µm), which could effectively reduce the sample dispersion and speed up the solution displacement as mentioned.

Analytical Application of the Sensor for Real Samples

To evaluate the practical application potential of the proposed sensor, the pH of some water samples including tap water, purified water and green tea water were determined under the same conditions. The green tea water samples were filtered before measurement and the other samples were detected directly. The obtained results are listed in Table 2 and compared with the data obtained by using commercial pH meter. It can be seen that all the results were in good agreement with those obtained by glass electrode method, indicating that the proposed sensor is acceptable for practical use.

Conclusion

A novel small-volume fiber-optic evanescent-wave pH sensor was successfully developed based on flow-injection analysis and fluorescence intensity determination. By using a cheap LED as light source, the sensor was simply fabricated by inserting a decladded optical fiber into a transparent capillary tube and setting the detector on the side of the capillary and using. The developed sensor exhibited following characteristics. First, the fabricated microchannel with narrow d_c (115 µm) of the sensor could reduce the sample dispersion caused by solution mixing, which finally enhanced the sensor sensitivity. Second, the small detection volume of 2.5 µL could speed up the solution displacement, leading to a short response time. Third, the sensor proposed here will be really useful for biography fluids detection, or enzyme-immunometric assay or toxicity test, since it needs small sample volume. Forth, the consumption of sensing reagent could be reduced

Table 2 Determination of pH values in real water samples

Sample	pH[a]	pH[b] (RSD (%))	Relative error[c] (%)
Purified water	7.05	7.12 (1.1)	0.9
Tap water	6.61	6.53 (1.9)	1.2
Green tea water 1	6.79	6.92 (2.3)	1.9
Green tea water 2	7.12	7.04 (1.6)	1.1
Green tea water 3	6.85	6.89 (3.2)	0.6

[a] pH value measured by the conventional glass electrode

[b] pH value measured by the proposed sensor, as the average of three determinations

[c] The relative error between pH value obtained by the proposed sensor and the glass electrode

significantly compared with normal size sensor. In addition, the configuration of the sensor provides a platform for monitoring other species by simply changing the light source and sensing reagents. The pH determination in real water samples showed good potential of practical applications of the sensor.

References

1. Grant SA, Glass RS (1997) A sol-gel based fiber optic sensor for local blood pH measurements. Sens Actuators B Chem 45:35–42
2. Pang P, Gao X, Xiao X (2007) A wireless pH sensor using magnetoelasticity for measurement of body fluid acidity. Anal Sci 23:463–467
3. Badugu R, Rostov Y, Rao G (2008) Development and application of an excitation ratiometric optical pH sensor for bioprocess monitoring. Biotechnol Prog 24:1393–1401
4. Epoy JPN, Lesniewska E (2007) Nano-pH sensor for the study of reactive materials. Anal Chem 79:7560–7564
5. Carter J, Alvis R, Brown S, Langry K, Wilson T, McBride M, Myrick M, Cox W, Grove M, Colston B (2006) Fabricating optical fiber imaging sensors using inkjet printing technology: a pH sensor proof-of-concept. Biosens Bioelectron 21:1359–1364
6. Safavi A, Maleki N, Rostamzadeh A, Maesum S (2007) CCD camera full range pH sensor array. Talanta 71:498–501
7. Seki A, Katakura H, Kai T (2007) A hetero-core structured fiber optic pH sensor. Anal Chim Acta 582:154–157
8. Ang P, Chen W, Wee A, Loh K (2008) Solution-gated epitaxial graphene as pH sensor. J Am Chem Soc 130:14392–14393
9. Ayad MM, Salahuddin NA, Abou-Seif AK, Alghaysh MO (2008) pH sensor based on polyaniline and aniline-anthranilic acid copolymer films using quartz crystal microbalance and electronic absorption spectroscopy. Polym Adv Technol 19:1142–1148
10. Dong S, Luo M, Peng G, Cheng W (2008) Broad range pH sensor based on sol-gel entrapped indicators on fibre optic. Sens Actuators B Chem 129:94–98
11. Turel M, Cajlakovic M, Austin E, Dakin JP, Uray G, Lobnik A (2008) Direct UV-LED lifetime pH sensor based on a semipermeable sol-gel membrane immobilized luminescent Eu^{3+} chelate complex. Sens Actuators B Chem 1:247–253
12. Gao W, Song J (2009) Polyaniline film based amperometric pH sensor using a novel electrochemical measurement system. Electroanalysis 21:973–978
13. Harbuzaru BV, Corma A, Rey F (2009) A miniaturized linear pH sensor based on a highly photoluminescent self-assembled europium (III) metal-organic framework. Angew Chem 48:6476–6479
14. Chen H, Wang X, Song X, Zhou T, Jiang Y, Chen X (2010) Colorimetric optical pH sensor production using a dual-color system. Sens Actuators B Chem 146:278–282
15. Xu B, Zhang WD (2010) Modification of vertically aligned carbon nanotubes with RuO$_2$ for a solid-state pH sensor. Electrochim Acta 55:2859–2864
16. Noire MH, Bouzon C, Couston L, Gontier J, Marty P, Pouyat D (1998) Optical sensing of high acidity using a sol-gel entrapped indicator. Sens Actuators B Chem 51:214–219
17. Qin W, Obare SO, Murphy CJ, Angel SM (2002) A fiber-optic fluorescence sensor for lithium ion in acetonitrile. Anal Chem 74:4757–4762
18. Busse S, Scheumann V, Menges B, Mittler S (2002) Sensitivity studies for specific binding reactions using the biotin/streptavidin system by evanescent optical methods. Biosens Bioelectron 17:704–710
19. Vogt F, Karlowatz M, Jakusch M, Mizaikoff B (2003) The automated sample preparation system MixMaster for investigation of volatile organic compounds with mid-infrared evanescent wave spectroscopy. Analyst 128:397–403
20. Keller BK, DeGrandpre MD, Palmer CP (2007) Waveguiding properties of fiber-optic capillaries for chemical sensing applications. Sens Actuators B Chem 125:360–371
21. Xiong Y, Xu J, Wang J, Guan Y (2009) A fiber-optic evanescent wave sensor for dissolved oxygen detection based on novel hybrid fluorinated xerogels immobilized with [Ru(bpy)$_3$]$^{2+}$. Anal Bioanal Chem 394:919–923
22. Xiong Y, Zhu D, Duan C, Wang J, Guan Y (2010) Small-volume fiber-optic evanescent-wave absorption sensor for nitrite determination. Anal Bioanal Chem 396:943–948
23. Xiong Y, Zhu D, Chen S, Peng H, Guan Y (2010) A fiber-optic evanescent wave O$_2$ sensor based on Ru(II)-doped fluorinated ORMOSILs. J Fluoresc 20:269–274
24. Xiong Y, Xu J, Zhu D-Q, Duan C-F, Guan Y-F (2010) Fiber-optic fluorescence sensor for dissolved oxygen detection based on fluorinated xerogel immobilized with ruthenium (II) complex. J Sol Gel Sci Technol 53:441–447
25. Lakowicz JR (1999) Principles of fluorescence spectroscopy, 2nd edn. Kluwer/Plenum, New York
26. Peterson JI, Vurek GG (1984) Fiber-optic sensors. Science 224:123–127
27. Ma LY, Wang HY, Xie H, Xu LX (2004) A long lifetime chemical sensor: study on fluorescence property of fluorescein isothiocyanate and preparation of pH chemical sensor. Spectrochim Acta A 60:1865–1872
28. Snee PT, Somers RC, Nair G (2006) A ratiometric CdSe/ZnS nanocrystal pH sensor. J Am Chem Soc 128:13320–13321
29. Jin T, Sasaki A, Kinjo M, Miyazaki J (2010) A quantum dot-based ratiometric pH sensor. Chem Commun 46:2408–2410
30. Westerlund F, Hildebrandt CB, Srensen TJ, Laursen BW (2010) Trihydroxytrioxatriangulene-an extended fluorescein and a chtungtrenung ratiometric pH sensor. Chemistry 16:2992–2996
31. Saleh NI, Al-Soud YA, Nau WM (2008) Novel fluorescent pH sensor based on coumarin with piperazine and imidazole substituents. Spectrochim Acta A 71:818–822
32. Cajlakovic M, Lobnik A, Werner T (2002) Stability of new optical pH sensing material based on cross-linked poly(vinyl alcohol) copolymer. Anal Chim Acta 455:207–213
33. Unciti-Broceta A, Yusop MR, Richardson PR (2009) A fluorescein-derived anthocyanidin-inspired pH sensor. Tetrahedron Lett 50:3713–3715
34. Zhang X, Rehm S, Safont-Sempere MM (2009) Vesicular perylene dye nanocapsules as supramolecular fluorescent pH sensor systems. Nat Chem 1:623–629
35. Maccraith BD, Mcdonagh C, O'Keeffe G, Butler BOKT, Mcgilp JF (1994) Fiber optic chemical sensors based on evanescent wave interactions in sol-gel-derived porous coatings. J Sol Gel Sci Technol 2:661–665